

Research Article

Antimicrobial Properties of Nanofiber Membrane and Commercial Micromembrane by Modification with Diethylenetriamine (DETA) and Attachment of Silver Nanoparticles

Izabela J. Gallus , Evren Boyraz , and Jiří Maryška

Faculty of Mechatronics, Informatics and Interdisciplinary Studies, Technical University of Liberec, Studentska 1402/2, Liberec 46117, Czech Republic

Correspondence should be addressed to Izabela J. Gallus; izabela.gallus@tul.cz

Received 12 October 2022; Revised 6 April 2023; Accepted 11 May 2023; Published 1 June 2023

Academic Editor: Wenhui Zeng

Copyright © 2023 Izabela J. Gallus et al. This is an open access article distributed under the Creative Commons Attribution License, which permits unrestricted use, distribution, and reproduction in any medium, provided the original work is properly cited.

Water demand is steadily increasing, and usable water supply is constantly decreasing. It is urgent to find a cheap and efficient way to recycle water. Currently, membrane technologies are getting promising results, but some factors drastically reduce their effectiveness. In membrane filtration, biofouling is one of the most limiting factors, reducing filtration efficiency. In this work, the micro- and nanofibres-composed membranes were modified with diethylenetriamine (DETA), and silver nanoparticles were attached to a modified surface to minimize biofouling risk during filtration. Different conditions were tested for reaction with DETA and attachment of nanoparticles. Antimicrobial tests were performed, and the leaching of nanoparticles over time was checked. The modified membranes (Nadir[®] MV020T and PA PVDF) containing silver nanoparticles ranging in size from 20 to 50 nm showed antibacterial properties against *Escherichia coli* in the form of 3–4 mm inhibitory zones. The percentage of released AgNPs was 0.47% and 2.12% for Nadir[®] MV020T and PA PVDF membrane after 21 days, respectively. Polyvinylpyrrolidone was used to increase the stability of the nanoparticles, and the results were compared.

1. Introduction

According to new UNICEF statistics, about 2 billion people suffer from scarcity of drinkable water [1]. Additionally, the demand for freshwater by the food and energy industries is increasing due to the growing population. Increasing droughts, unsustainable groundwater extraction, and inadequate water infrastructure also contribute to the increased demand for fresh water. For this reason, it is crucial to find an easy and economical way to treat and reclaim water [2]. Although 70% of the world is covered with water, there is a severe lack of drinking water in many countries. Approximately 97.5% of the earth's water is salty water found in the oceans. The remaining 2.5% is freshwater, such as groundwater, icebergs, lakes and rivers, serving the most needs of humans and animals [3, 4]. The water consumption rate every 20 years exceeds twice the population growth rate and raises concerns about dwindling water resources

worldwide [5]. Various industrial and developmental activities have caused the recent increasing pollution and deterioration of water quality. Therefore, water treatment is becoming more critical for world countries to tackle water scarcity by strengthening their infrastructure with increased global freshwater consumption. In recent years, many types of membranes have been produced and tested for water treatment.

Considering the effective membrane properties of nanofiber technology, it offers advantages for separation technology as follows:

- (i) High surface area to volume ratio.
- (ii) A highly porous and narrow pore size of the nanofibers allows good selectivity.
- (iii) Surface can be modified easily.
- (iv) Many types of polymeric solutions can be used for the preparation of nanofibers.

- (v) The nanofibers' highly interconnected and asymmetric structure may reduce the fouling [6, 7].

Awareness of water and wastewater treatment will increase with increasing amounts of waste and decreasing water resources worldwide, and the market for membrane separation technology will grow in the industry. The membrane separation technology market was valued at USD 22.70 billion in 2019, and the membrane separation technology market is expected to grow rapidly. It is projected to grow at a compound annual growth rate of 7.30% from 2020 to 2027 to reach USD 38.34 billion by 2027 [8].

Membrane filtration is one of the most effective and economical technologies for water treatment. Polymeric membranes that show potential in water treatment are made from polysulfone, polypropylene, polyvinylidene fluoride (PVDF), and polyether sulfone because they have adequate chemical and physical resistance and low cost of large-scale production [9]. The limiting factor in the effectiveness and efficiency of membrane techniques is fouling, which includes inorganic scaling, colloidal fouling, organic fouling, and biofouling [10]. They contribute to reducing filtration efficiency by decreasing water flow and reducing membrane lifespan by irreversibly blocking the membrane pores [11, 12]. Among them, biofouling is considered the most fatal. Biofilm formed on the membrane's surface is hard to remove, and chemical cleaning is often not enough [13]. Numerous studies have been conducted to reduce or eliminate biofouling during membrane processes. Attempts have been made to alter membrane surface properties by changing hydrophilicity, surface charge, or surface roughness [14–16]. For example, Khoerunnisa et al. [17] created a polyethersulfone membrane using phase inversion, which was then immersed in CS/NH₄Cl, obtaining antibacterial properties of the membrane against *Staphylococcus aureus* and *Escherichia coli* getting bactericidal killing ration value of 99.2% and 83.3%, respectively. Peer et al. [18] improved the hydrophilicity and antimicrobial properties of a PVDF-co-hexafluoropropylene nanoporous membrane by adding a medium chain of 1-monoacylglycerols. One method to obtain additional properties of materials is to attach and integrate into the material surface various molecules or compounds with desired properties that the modified material surfaces would have [19]. To ensure the stability of the attached components to the modified materials and to prevent the materials from losing their newly acquired properties, it is important that the resulting interaction between the two components be long-lasting and difficult to break. Among the most durable interactions are chemical bonds, particularly covalent bonds [20]. By attaching new elements to a surface, it is necessary to consider the accompanying chemistry. Agents with antibacterial properties include various types of nanoparticles such as CuO [9, 21], TiO₂ [9, 22], ZnO [9, 23], Al₂O₃ [24], Fe₃O₄ [25], and Ag [9, 26]. During the attachment of nanoparticles to a surface, it is necessary to take into account their affinity for different functional groups (see Figure 1). Three main groups of nanoparticles can be distinguished. The first includes noble metals (e.g., Ag or Au), which are usually functionalized with thiol groups, but also with amine or cyanides. The second group includes oxides, where oxygen can form bonds with

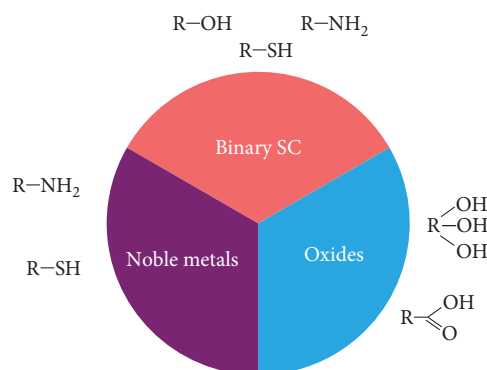


FIGURE 1: Common functional groups are used for NPs functionalization according to their affinity [27].

hydroxyl groups. Binary compounds are recognized as the third group, and this group primarily includes elements from groups 12 to 16, which are components of fluorescent semiconductor NPs. Thiol, hydroxyl, and amine groups are commonly used for their binding [27].

Silver nanoparticles are widespread due to their easy preparation, high antibacterial activity, and unique biological, chemical, and physical properties [28]. Their small size and large surface area exhibit activity not only against bacteria but also viruses and fungi [29, 30]. Silver nanoparticles with a size of 1–10 nm are considered the most effective and active against pathogens [31]. The exact mechanism of action of AgNPs against pathogens is unknown, although it is known to be due to the synergistic action of both Ag⁺ ions and Ag⁰ nanoparticles [32]. They cause the formation of free radicals and, thus, oxidative stress in the bacterial cell [9, 26, 32]. Silver nanoparticles have a high affinity for functional groups such as amine, carbonyl, phosphate, and sulfhydryl. These are the building blocks for many key cell compounds, i.e., proteins, enzymes, or DNA [33–35]. The binding of silver nanoparticles to these cellular elements can lead to changes in the structures of these elements and irreversible damage, eventually leading to apoptosis or cell death [36].

When designing materials containing silver nanoparticles, it is essential to consider issues regarding their safety concerning humans. It is well known that we do not have a full guarantee that the use of nanoparticles is entirely safe. However, there is insufficient evidence stating that their use is unsafe. According to WHO, no greater than 0.1 mg/mL of silver in drinking water is said to be acceptable and is present in the form of silver ions at +1 oxidation state and nanoparticles [37]. Moreover, silver nanoparticles are commonly used in daily objects such as shampoos, sprays, toothpaste formulations, food packing composites, or wound dressings. On the other hand, in some fields, the use of nanoparticles is limited by legalization permission protocols that must be granted before a product can enter public use. However, there are no internationally agreed testing standards for nanomaterials. Currently, International Standards Organization (ISO) has introduced guidelines (ISO TC 229) relying on information and labeling of nanoproducts to make customers aware of what they are buying [38].

Nonetheless, the continued growth of industry interest in silver nanoparticles and rapid development will force the introduction of new regulations and means of standardization. Continuous research is being conducted to determine the effects of nanomaterials on human health [39]. Moreover, it is essential to remember that AgNPs have good chemical stability, high conductance, catalytic activity, and high field enhancement, making them one of the best potential nano-based materials for wastewater treatment [40].

In this research, a nanofiber PVDF membrane (PA PVDF) and a commercially available micromembrane Microdyn Nadir[®] MV020T were modified in diethylenetriamine (DETA) solution to obtain functional amine groups, which were later used as anchors for silver nanoparticles. Silver nitrate was used as a precursor for silver ions, and reduction was performed using different concentrations of ascorbic acid. To confirm the antibacterial properties of the modified membranes, antibacterial tests against *E. coli* were performed, with positive results. Analyses were carried out to compare the modified membranes with their original forms and determine the changes in their chemical and physical properties. In addition, the effect of polyvinylpyrrolidone (PVP) on the size of the obtained nanoparticles and their antibacterial properties was checked.

2. Materials

In this research, two types of membranes were modified. One type of them was a commercial flat sheet, and another was a nanofibrous membrane. Commercially available microfiltration membrane NADIR[®] MV020T made from PVDF with a nominal pore size of 0.2 μm was provided by Mann + Hummel (Germany). PA PVDF nanofiber membrane was designed and developed at the Technical University of Liberec, Czech Republic. PA PVDF consists of three layers, electrospun PVDF nanofibers on top, polyethylene terephthalate support at the bottom, and adhesive polyamide (PA) web in the middle. The layers were combined by heat-press lamination. Membranes were washed before and after modification with deionized water and ethanol. The modification was done in a DETA aqueous solution provided by Sigma Aldrich, Germany. Silver nanoparticles were obtained by reducing silver nitrate ($\text{AgNO}_3 > 99\%$) in ascorbic acid, which was purchased from Sigma Aldrich, Germany. To improve the stability of the nanoparticles, PVP (58,000 M.W.) was used and provided by Alfa Aesar, Germany. Antimicrobial testing was performed using an *E. coli* strain (MG1655).

3. Methods

3.1. Surface Modification with DETA. The membranes were washed with ethanol and deionized water before modification to clean the surface and remove all impurities. The reaction was carried out in aqueous 4 M DETA solution under different conditions of time and temperature. The reaction was performed at 40, 60, and 80°C and in time 1, 3, and 5 hr, according to Table 1. The membranes were washed again after the reaction. The presumed mechanism of the reaction is shown in Figure 2. The strong alkaline environment initiates a reaction to eliminate fluorine from

TABLE 1: Tested reaction conditions with diethylenetriamine.

Membranes	Reaction temperature (°C)	Time (hr)	The concentration of DETA (M)
MV020T, PA PVDF	80	1	4
		3	
		5	
	60	1	4
		3	
		5	
	40	1	4
		3	
		5	

the polymer chain, resulting in a carbon atom missing one bond. In this case, either a double bond can be formed between the carbon atoms, or the nitrogen atom can attach from DETA.

3.2. Delamination Test. The bursting test determined the changes in the mechanical properties of membranes that had a place with progressing reaction time. The test measured the hydrostatic pressure at which the membrane layers detached from each other. The membranes under test were placed between two metal rings tightly fitted to each other and locked together once the membrane was seated. Pressurized water flowed through the closed system, with the pressure increasing with time. When the membrane delaminated, the pressure dropped dramatically, and the maximum pressure prior to delamination was noted as the bursting strength of the membrane.

3.3. Silver Nanoparticles (AgNPs) Incorporation. Washed and modified membranes were placed in 3.5% AgNO_3 for 4 hr. After this time, the membranes were rinsed and immersed in ascorbic acid for 3 hr. The size of the silver nanoparticles obtained was controlled by the concentration of ascorbic acid [41, 42]. The desired size of AgNPs was less than 100 nm. In order to obtain nanoparticles smaller than 100 nm, it was checked how the concentration of ascorbic acid used affected the size of the obtained nanoparticles. The size of the resulting nanoparticles was checked at reducing agent concentrations of 4, 6, 8, and 10 wt%. In addition, the effect of the surfactant PVP on the size, shape, and antibacterial properties of silver nanoparticles was checked. For this purpose, 10 wt% ascorbic acid was prepared in two separate beakers, and 1 wt% PVP was added to one of them. The conditions for all other reactions to follow remained the same as for the reaction described earlier.

3.4. Membrane Characterization. In order to recognize the changes that occurred on the surface and in the structure of the modified membranes, pore size measurements were made, and scanning electron microscopy (SEM) and Fourier transform infrared spectroscopy (FTIR) were used. The pore size of the membranes was checked using the bubble point method by Porometer 3G through a pore size analyzer (Quantachrome Instruments, Anton Paar GmbH).

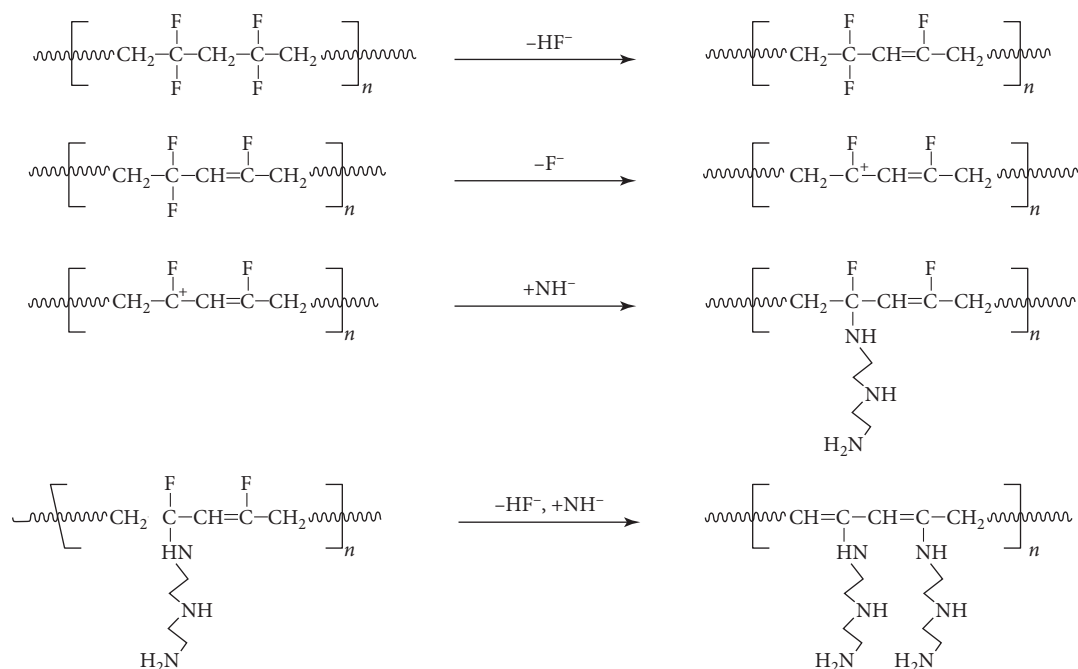


FIGURE 2: The predicted reaction mechanism between the PVDF membrane surface and diethylenetriamine (DETA).

The Vega 3SB SEM and Zeiss Ultra Plus with energy dispersive spectroscopy (EDS) Oxford Instruments X-Max were used to visualize a membrane surface and to check nanoparticle size and their distribution on the surface at the Technical University of Liberec, Czech Republic. The samples were covered with a 7 nm gold layer before the observation. Some pictures were taken by Quanta 650 FEG SEM at the Catalan Institute of Nanoscience and Nanotechnology (ICN2, Barcelona, Spain). ImageJ program (National Institute of Health, USA) was used to calculate the size of obtained silver nanoparticles. The infrared spectroscopy was measured by Nicolet iZ10 FTIR (Thermo Scientific, Prague, Czech Republic) in the range of 400–4,000 cm⁻¹ to estimate changes in chemical bondings.

3.5. Water Contact Angle. The contact angle for deionized water was checked before and after the modification to observe changes in the hydrophilicity of the membranes. See System E (version 7.6) from Advex Instruments (Czech Republic) was used to determine the contact angle. 3 μL of distilled water was carefully applied to the surface of the membranes, and the image was captured after stabilizing the water droplet. The program calculated the contact angle between the membrane surface and the droplet. Measurements were taken in five different places on the membrane, and the average contact angle was calculated. The measurements were made at room temperature.

3.6. Antibacterial Test of Modified Membranes. Antimicrobial testing was performed using AATTCC Method 147 [43] by checking the inhibitory zones. A single *E. coli* colony was transferred to the sterilized broth and incubated for 24 hr at 37°C. The modified membranes were sterilized under UV light (λ = 254 nm) for 1 hr. The membranes were placed on agar plates. Four bacterial suspensions were prepared from

previously established cultures containing 10⁸, 10⁷, 10⁶, and 10⁵ live cells per 1 mL solution (CFU/mL), respectively. Bacterial solutions were linearly applied to the membranes and incubated for another 24 hr.

3.7. Permeability. The permeability of the original and modified membranes was measured in an Amicon model 52 stirred filtration cell with a volume of 50 mL and a filtration area of 13.4 cm² (Merck Millipore, Germany). The test was conducted for 100 min at room temperature and at a constant transmembrane pressure of 1.0 bar. The deionized water flow continuously in dead-end mode, stirred above the membrane.

3.8. Leaching Test. The stability of the silver nanoparticles was verified, and the number of nanoparticles released from the membrane was determined by the leaching test. The modified membranes were placed vertically in a beaker containing 100 mL of distilled water and placed on a magnetic stirrer setting the speed to 150 rpm for 21 days. A 5 mL water sample was taken after 2, 4, and 8 hr and after 1, 3, 7, 14, and 21 days. After the test was completed, the membrane was cut into smaller pieces and placed in 10 mL of 68% nitric acid for 15 hr. The appropriate dilution was then adjusted, and the Ag ion concentration was determined. All samples were measured on inductively coupled plasma mass spectrometry analysis (ICP-MS) NexIon 300D, Perkin Elmer (USA). All measurements of nanoparticles amount were established by the ICP-MS method.

4. Results and Discussion

4.1. Optimization of Reaction Conditions for DETA Modification and Mechanical Properties of Modified Membranes. Early observations suggested that the longer the reaction time and higher

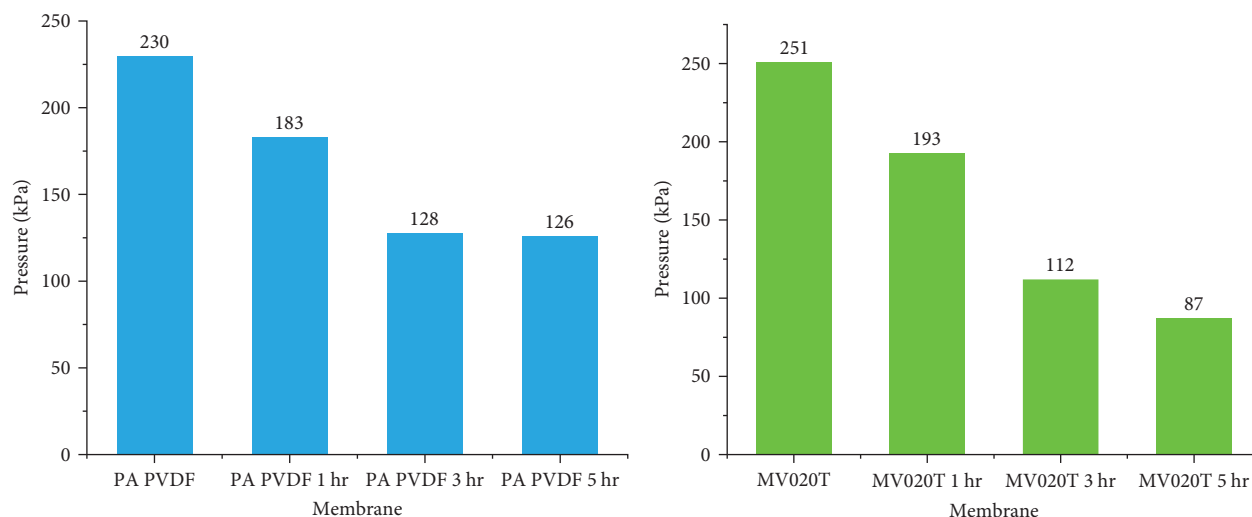


FIGURE 3: The bursting pressure required to delaminate membranes modified at different times at 80°C.

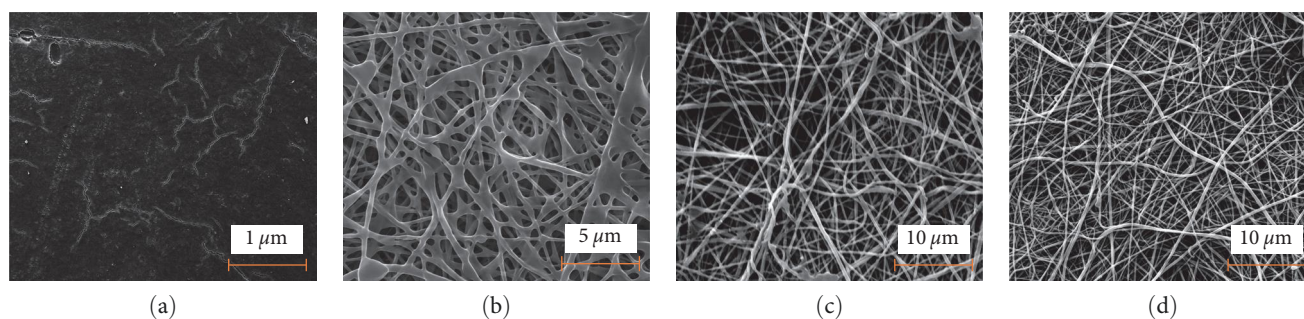


FIGURE 4: Surface of (a) MV020T membrane (magnification $\times 97$) and (b) PA PVDF (magnification $\times 10k$) that were modified 5 hr at 80°C. Nanofibers of PA PVDF membrane (c) after reaction carried out at 3 hr in 60°C (magnification $\times 13k$) and (d) after reaction carried out at 3 hr in 80°C (magnification $\times 7k$).

the temperature, the more significant the reaction progress. This was indicated by the color of the membranes, which changed from white to light brown, then to dark brown, and finally to nearly black. The membranes became increasingly brittle and fragile as the reaction time and temperature increased. It was decided to conduct a delamination test for different reaction times at the highest temperature tested to confirm whether the observed changes are reflected in reality. Analyzing the results, it is clear that the modification weakens the membranes' mechanical properties. After 1 hr of the reaction, the required hydrostatic pressure for membrane layers delamination was reduced by 20.4% and 23.1% for PA PVDF and MV020T, respectively. The longer the response time, the lower the hydrostatic pressure required. A further progression of reactions results in a decrease of 44.3% and 45.2% for the nanofibers membrane and 55% and 65.3% for the flat sheet membrane after 3 and 5 hr, respectively. Figure 3 illustrates the changes in bursting pressure with the increased reaction time. It shows that the optimum reaction time cannot be too long, as the reaction will cause irreversible damage to the strength of the membranes, which is essential when conducting filtration.

To better understand why membranes lose strength, it was examined how the membrane surface looks after modifications.

When the reaction was carried out at the highest tested values, i.e., for 5 hr and at 80°, the formation of cracks can be observed on the surface of the MV020T membrane, which certainly also affected the drastic decrease in the mechanical properties of the membrane (Figure 4(a)). Too long a reaction time and too high a temperature also affect the structure of nanofibres. As the temperature and reaction time increase, the average diameter of the nanofibres increases. The average diameter of the nanofibres after the reaction increased from 180 to 185, 192, and 200 nm for the reaction carried out at 40, 60, and 80°C, respectively. The nanofibres lose their previous shape when this reaction is carried out for 5 hr. Very long exposure to an alkaline environment causes deformation and dissolves the PVDF nanofibres (Figure 4(b)). That causes the weakening of the membrane's mechanical properties and ultimately leads to membrane's layers delamination.

FTIR analysis was carried out to check whether the membrane structure had changed and to examine the chemical composition of the membranes.

The FTIR results are shown in Figure 5. The presence of $-\text{NH}$, $-\text{CF}$, $-\text{C}=\text{C}$, and $\text{C}=\text{O}$ groups is essential to estimate the changes in PVDF membrane structure and if the reaction occurred. FTIR analysis for reactions carried out at 40 and

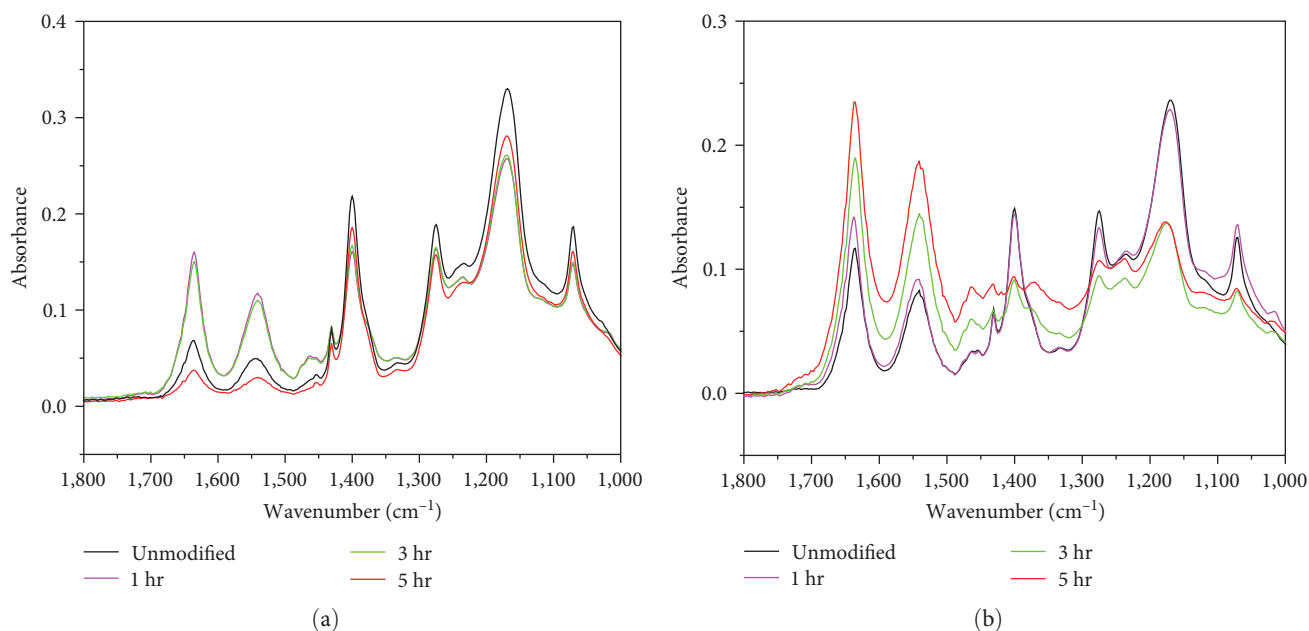


FIGURE 5: Fourier transform infrared spectroscopy (FTIR) spectra of PA PVDF membrane surface after modification in DETA for 1, 3, and 5 hr in (a) 60°C and (b) 80°C.

60°C (Figure 5(a)) showed no change in the material structure. Therefore, it can be inferred that those temperatures were not sufficient to initiate the reaction. However, changes can be seen in samples modified at 80°C (Figure 5(b)). The resulting spectrum for the sample modified for 1 hr is very comparable to the unmodified sample. It can therefore be assumed that also 1 hr of reaction at 80°C did not cause a reaction. After 3 and 5 hr, the intensity of peaks corresponding to bi-halide oscillations, which can be observed between 1,050 and 1,250 cm^{-1} , decreases significantly. It may indicate that fluorine is gradually eliminated from the polymer chain and replaced with new bonds. Reading the new peaks from primary and secondary amines is made much more difficult due to the presence of PA in the adhesive layer. The spectra show the presence of peaks from the primary amine at 1,550 and the secondary amine in the range 1,630–1,680 cm^{-1} . It is important to remember that FTIR is not a quantitative method in this case, only a qualitative one. However, such a significant difference in peak intensity may be indicative of a larger number of amine groups in the modified samples. In this range (1,600 cm^{-1}), the signals from the stretching vibrations of the conjugated C=C groups should also be visible if the reaction occurs, according to Figure 2. However, vibrations from the amines make them impossible to observe. Instead, changes in the deformation vibrations of the $-\text{CH}_2-$ groups adjacent to the fluorine-linked carbon atom can be observed. In the pristine sample and the sample modified for 1 hr, the intensity of the peak of this group at wavelength 1,400 cm^{-1} is clear and strong, while for the samples modified for 3 and 5 hr, their visibility and intensity decreased significantly. This may indicate that this is due to the transition of the $-\text{CH}_2-$ group into $-\text{CH}=\text{C}-$.

After analyzing all the results that were obtained, a reaction carried out at 80°C for 3 hr was chosen as the optimal

condition for this modification. The reactions at lower temperatures (40 and 60°C) were insufficient to eliminate fluorine and attach the amine group to the membrane surface. Even a long treatment time did not allow the reaction to proceed in these cases. The reaction at 80°C and for 5 hr weakened the membrane's mechanical properties too much to be used successively in water filtration. In contrast, the reaction carried out for 1 hr at this temperature was not long enough to observe changes in the FTIR spectrum. The long reaction time causes the membranes to become brittle, and a too-low temperature does not initiate the reaction. The membrane modified at 80°C for 3 hr has good mechanical properties and visible changes in structure. Further experiments were performed on membranes modified in those conditions.

4.2. Membrane Wettability. Many previous studies have shown that the high surface hydrophilicity decreases the intensity of biofouling, improves water filtration parameters, and reduces waste water filtration energy costs [44–46]. The measurement of the contact angle helped to evaluate the changes in the wetting properties of the membranes. The initial contact angle of PA PVDF was 102°, 9°, and it was noted that with increasing modification time, the hydrophilicity of the membrane increased. Initially, the contact angle value decreased to 45°, 4° after 1 hr, eventually reaching 0° after 3 and 5 hr of reaction (Figure 6). The modification also improved the hydrophilic properties of the MV020T membrane surface. Initially, the contact angle was 34°, 8°, and after the modification, its value decreased to 0° regardless of the reaction conditions. This shows that the performed modification contributes to an increase in the hydrophilicity of the membrane surface and thus can lead to fouling reduction during filtration.



FIGURE 6: Contact angle measurement for pristine (a) and modified (b) 1 hr PA PVDF membrane.

4.3. Attaching Silver Nanoparticles. The step involving the reduction of silver ions to nanoparticles was carried out using different concentrations of ascorbic acid, i.e., 4, 6, 8, and 10 wt%. It was observed that the higher the concentration of the reducing agent used, the smaller the size of the nanoparticles obtained. By low concentration of ascorbic acid, silver nanoparticles appeared likely as agglomerates rather than individual particles. The reason for this behavior may be the faster consumption of silver ions through their adsorption by oxidation products, resulting in reduced time for growth and the formation of larger agglomerates. Similar results were obtained in the work of Janah et al. [47], where the effect of ascorbic acid concentration on the properties of silver nanoparticles was studied, and in the work of Jain et al. [48], where the synthesis and control of the size and applications of copper nanoparticles were described. He et al. [49] studied the effect of various parameters on the size of silver nanoparticles. According to their study, the reducing activity of the reducing agent significantly affects the size of the obtained nanoparticles. The higher the reducing activity, the smaller the nanoparticles can be obtained. Silver nanoparticles formed using ascorbic acid at concentrations of 6 and 8 wt% were deposited on the membrane uniformly and individually and formed agglomerates only in single places. All AgNPs were obtained in spherical form. The average size of nanoparticles using 4 wt% ascorbic acid was 130 nm, 6 wt%—80 nm, and 8 wt%—50 nm. The smallest nanoparticles were obtained when 10 wt% ascorbic acid was used. Their size was then about 46 nm. In addition, the effect of PVP surfactant on the size, shape, and distribution of silver nanoparticles was checked. Figure 7 shows images depicting silver nanoparticles on the surface of MV020T and PA PVDF membrane at a concentration of 10 wt% ascorbic acid in the presence and absence of surfactant.

The use of surfactant significantly affected the size and quantity of embedded nanoparticles. When surfactant was used, the amount of nanoparticles on the membrane relatively increased, and their size decreased. The PA PVDF membrane without added surfactant contained an average of 7,439.2 mg/kg of the membrane and with added surfactant 8,225.2 mg/kg. The average diameter size of AgNPs for the MV020T membrane when surfactant was used was 18.41 and 21.59 nm without it. For the PA PVDF membrane, the values were 46.31 and 53.03 nm, respectively. PVP is widely

used as a stabilizer for silver nanoparticles due to its low toxicity, water solubility, biodegradability, biocompatibility, and temperature resistance. The high affinity of PVP for AgNPs is due to the presence of oxygen and nitrogen atoms. It behaves as a capping agent through the spherical and electrostatic stabilization provided by the amide groups present in the pyrrolidine ring. PVP prevented agglomeration of the nanoparticles and reduced their resulting size by forming a capping layer around the nanoparticles [50, 51]. It should be mentioned that too high a concentration of PVP will lead to an increase in nanoparticles rather than a decrease [41]. Therefore, an appropriate concentration of PVP had to be selected to obtain smaller nanoparticles and preserve their antibacterial properties.

To confirm that the particles obtained were silver nanoparticles, EDS analysis was additionally performed. Table 2 shows the atomic weight results obtained for the modified membranes. Also, this analysis shows that the silver content on the membranes was higher when a surfactant was used.

4.4. Membranes Pore Size. The measurement of pore size was conducted after AgNPs attachment. The average pore size of the PA PVDF membrane was initially $0.615\ \mu\text{m}$, and after modification decreased to $0.282\ \mu\text{m}$. The largest pore size was also reduced from 0.940 to $0.634\ \mu\text{m}$ after modification. The reason may be related to the increase in nanofiber diameter after modification. Enlarging the nanofibers significantly shrunk the free space between them, thus reducing the average and the largest pore size. The exact pore sizes for MV020T and PA PVDF membranes are shown in Figure 8.

For the MV020T membrane, both the value for the average and largest pore size increased. The effect of an alkaline environment on PVDF membranes was studied by Rabuni et al. [52]. According to their study, PVDF membranes can already be attacked and degraded at low sodium hydroxide concentrations of 0.01 M. The strongly alkaline reaction environment may have led to partial membrane degradation and enlargement of its pores.

4.5. Antibacterial Test of Modified Membranes. Antimicrobial tests were performed for membranes where 10 wt% ascorbic acid was used in the presence and absence of PVP surfactant. The results obtained after the antibacterial trial against *E. coli*

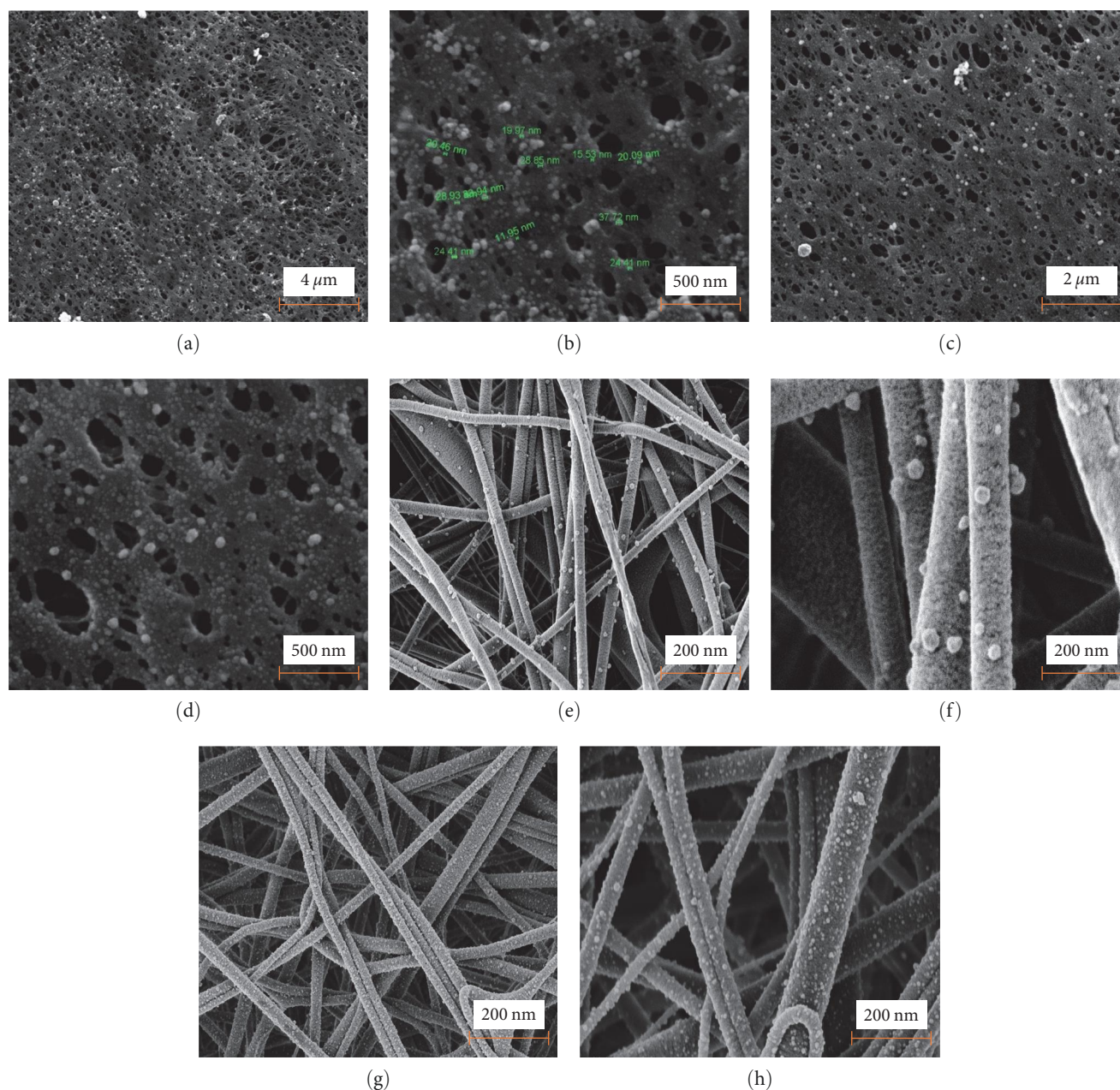


FIGURE 7: Silver nanoparticles on flat sheet MV020T membrane surface (a) (magnification $\times 27k$), (b) (magnification $\times 131k$) without using PVP, (c) (magnification $\times 48k$), (d) (magnification $\times 140k$) in the presence of PVP and PA PVDF membrane (e) (magnification $\times 25k$), (f) (magnification $\times 100k$) without using PVP, (g) (magnification $\times 25k$), (h) (magnification $\times 50k$) in the presence of PVP.

TABLE 2: Percentage of atomic EDS analysis for samples prepared with (+) and without (–) PVP.

Sample	C (%)	O (%)	F (%)	Si (%)	Ag (%)
MV020T PVP (–)	77.30	5.18	17.00	0.3	0.22
MV020T PVP (+)	72.64	8.18	17.15	1.74	0.28
PA PVDF PVP (–)	82.75	3.53	13.43	–	0.28
PA PVDF PVP (+)	83.64	4.45	10.54	–	1.38

for the original and modified PA PVDF and MV020T membranes are shown in Figure 9.

Both membranes modified in the presence and without surfactant showed strong antibacterial properties in the form

of inhibitory zones. In contrast, bacteria on the original membranes grow freely near the membrane as well as on the membrane itself. A PA PVDF membrane modified at 10 wt% without surfactant showed negligible antibacterial activity.

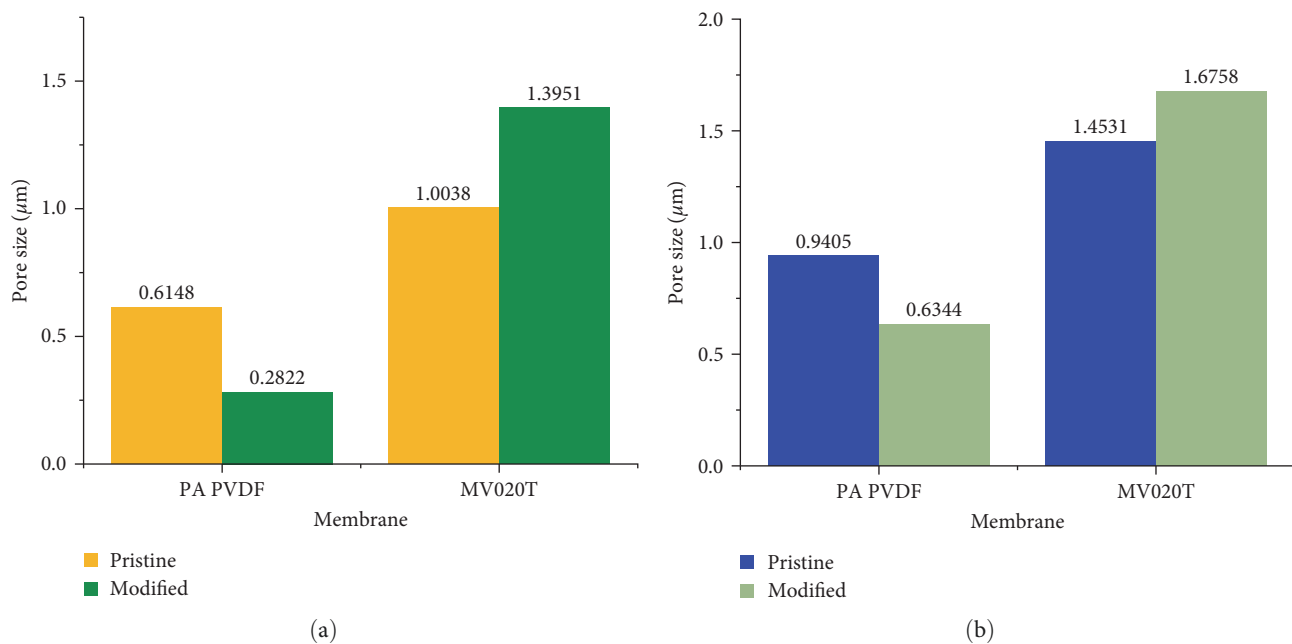


FIGURE 8: (a) Mean and (b) the biggest pore size for pristine and modified PA PVDF and MV020T membrane.

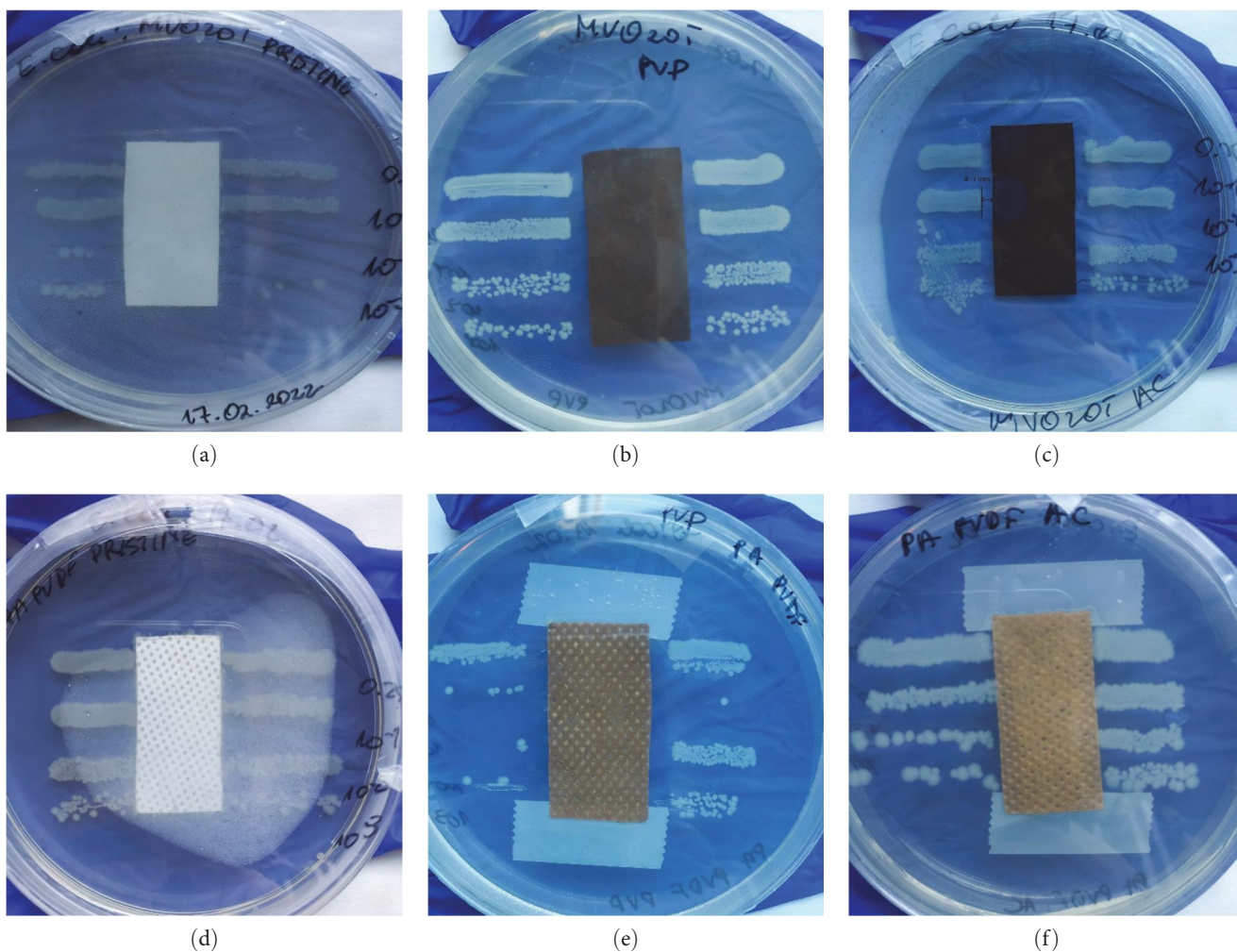


FIGURE 9: Antibacterial test for modified MV020T and PA PVDF membranes: (a) MV020T pristine membrane; (b) MV020T with PVP surfactant; (c) MV020T without surfactant; (d) PA PVDF pristine membrane; (e) PA PVDF with PVP surfactant; (f) PA PVDF without surfactant.

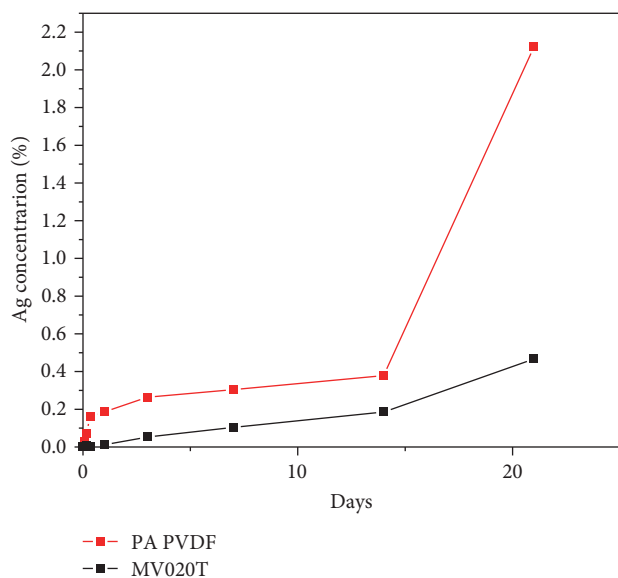


FIGURE 10: Leaching of AgNPs from PA PVDF and MV020T membranes over 21 days.

This suggests that the presence of surfactant improved the stability of the nanoparticles and facilitated their uptake by bacterial cells. The size of the inhibitory zones for the other modified membranes was about 3–4 mm. It is known that surfactant molecules subsequently adsorb onto the surface of the particles, promoting steric stabilization [53–55]. Their adsorption onto the surface of the nanoparticles prevents the formation of large nanoparticles by inhibiting their aggregation [56]. That led to smaller nanoparticles size and, ultimately, better antibacterial properties due to the size and distribution of silver nanoparticles. In addition, the positive effect of PVP on the antimicrobial properties of nanoparticles is explained by El-Kheshen and El-Rab [57], where they assume that the mechanism of the antimicrobial action of silver nanoparticles implies the disruption of the bacterial membrane by silver ions release from PVP. The Ag ions create insoluble compounds with the sulhydryl groups in the cell wall of the microorganism. The presence of amino groups in the PVP chain may induce Ag⁺ motions. The mechanism of Ag⁺ release is not explained, but it is speculated that the amino group improves Ag⁺/H⁺ ion exchange.

4.6. Releasing of AgNPs from Modified Membranes. The percentage of released nanoparticles after 21 days was 0.47% for MV020T membrane and 2.12% for PA PVDF membrane. This represents a very good result, as only a small percentage of nanoparticles are released into the environment. The total mass of nanoparticles on the membrane surface was 0.820 mg/cm² for MV020T and 0.183 mg/cm² for PA PVDF. The amount of AgNPs attached to the flat sheet membrane was almost 4.5 times higher than for the nanofiber membrane. The highest release of nanoparticles in both cases occurred after 14 days of testing. Figure 10 shows the percentage of the total released AgNPs mass from the membrane surface in 21 days. The biggest burst of AgNPs for PA PVDF reached 2.1% and appeared after 21 days of conducting the test. However, the

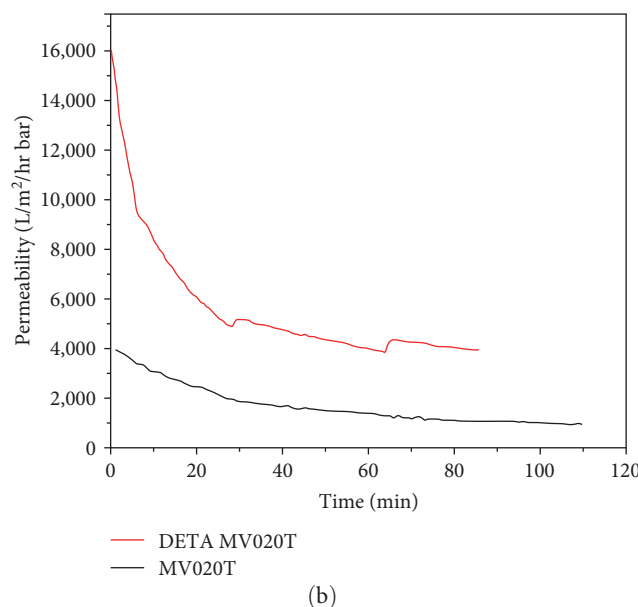
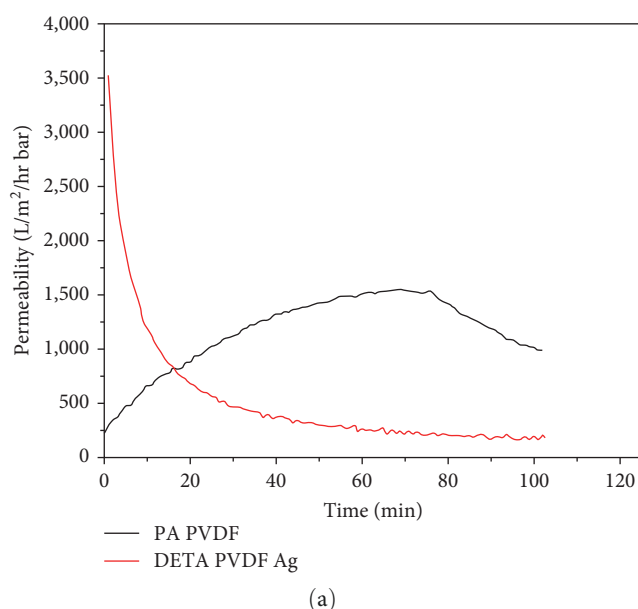


FIGURE 11: The water permeability of pristine and modified (a) PA PVDF and (b) MV020T membranes.

numerical value of this release is 0.003842 mg/cm² in the closed measurement system. This value, when running filtration with a continuous supply of fresh feed, will not significantly impact the environment and filtration process.

4.7. Filtration Parameters and Water Permeability. During filtration, the membrane composed of nanofibers is damaged, which can be recognized by the fact that water permeability increases with time. The modified PA PVDF membrane, on the other hand, does not behave this way. This indicates that the modification further protects the membrane from mechanical damage during filtration. However, water permeability should be improved for this membrane, as the water flux obtained was very slow. A graph showing water permeability over time can be observed in Figure 11.

In contrast, water permeability for the MV020T membrane has increased compared to the original membrane. However, it is important to note that the pore size of this membrane has increased, and therefore the separation capacity has also been changed.

5. Conclusion

In this study, a new method for surface modification of PVDF membranes has been developed. Optimal reaction conditions for modification with DETA have been determined. The best results were obtained for the reaction carried out for 3 hr at 80°C with a molar concentration of DETA of 4 M. The attached nanoparticles' size depended on the ascorbic acid concentration. According to the literature, the most effective bactericidal silver nanoparticles are those with a size of 1–10 nm, but antibacterial activity can also be observed for nanoparticles reaching a size of 100 nm. Using ascorbic acid at concentrations of 10 wt%, nanoparticles of about 46 nm in size were obtained. Adding PVP to a 10 wt% ascorbic acid reduced the resulting nanoparticle size, and particles of about 19 nm could be obtained on the MV020T membrane. This positively affected antimicrobial tests, during which the modified membranes showed strong antibacterial properties. The use of PVP surfactant gave an increase in the quantity of deposited nanoparticles and a decrease in their size. In addition, it resulted in relatively better antibacterial properties for the modified membranes. The percentage of released nanoparticles at 21 days was 0.47% for MV020T membrane and 2.12% for PA PVDF membrane, which is considered an excellent result. In addition, the modification plays a protective role for the membranes during filtration, which may contribute to an increase in membrane life. The subsequent research should focus on improving water permeability, especially for the PA PVDF membrane. The modification process attempted in the present work could also be tried on other PVDF surfaces to enhance their antibacterial properties potentially.

Data Availability

The datasets generated during and/or analyzed during the current study are available from the corresponding author upon reasonable request.

Conflicts of Interest

The authors declare that they have no conflicts of interest.

Acknowledgments

This work was supported by the Student Grant Competition of the Technical University of Liberec under project no. SGS-2021-3027. The authors acknowledge the assistance provided by the Research Infrastructure NanoEnviCz, supported by the Ministry of Education, Youth and Sports of the Czech Republic under project no. 2021-12-22. This work was supported by the Technology Agency of the Czech Republic in the framework of project no. FW01010306, Smart filtration of tertiary wastewater

treatment using hi-tech fabrics and nanofiber membranes, Czech Republic. The authors would like to extend their thanks to the research group Nanostructured Functional Materials led by Daniel Ruiz Molina in the Catalan Institute of Nanoscience and Nanotechnology in Barcelona (Spain), where part of the study was conducted and to Eduard Torrent for providing the bacterial *Escherichia coli* strain.

References

- [1] UNICEF DATA, “Progress on household drinking water, sanitation and hygiene, 2000–2020: five years into the SDGs,” UNICEF DATA, July 2021, <https://data.unicef.org/resources/progress-on-household-drinking-water-sanitation-and-hygiene-2000-2020/>.
- [2] P. Rogers and S. Leal, *Running Out of Water: The Looming Crisis and Solutions to Conserve Our Most Precious Resource*, St. Martin's Publishing Group, 2010.
- [3] R. Rajagopal, M. Wichman, and E. Brands, “Water: drinking,” in *International Encyclopedia of Geography: People, the Earth, Environment and Technology*, D. Richardson, N. Castree, M. F. Goodchild, A. Kobayashi, W. Liu, and R. A. Marston, Eds., John Wiley & Sons, Ltd., 2016.
- [4] M. Shatat and S. B. Riffat, “Water desalination technologies utilizing conventional and renewable energy sources,” *International Journal of Low-Carbon Technologies*, vol. 9, no. 1, pp. 1–19, 2014.
- [5] M. Tuninetti, S. Tamea, and C. Dalin, “Water debt indicator reveals where agricultural water use exceeds sustainable levels,” *Water Resources Research*, vol. 55, no. 3, pp. 2464–2477, 2019.
- [6] E. Boyraz, *Preparation of Nanofibrous Membranes for Oil/Water Separation*, Technical University of Liberec, https://dspace.tul.cz/bitstream/handle/15240/154223/BoyrazEvren_DP.pdf?sequence=1&isAllowed=y, 2019.
- [7] A. Gul, I. Gallus, A. Tegginamath, J. Maryska, and F. Yalcinkaya, “Electrospun antibacterial nanomaterials for wound dressings applications,” *Membranes*, vol. 11, no. 12, Article ID 908, 2021.
- [8] Markets and Markets, “Membrane separation technology market by application & region-global forecast 2022,” Markets and Markets, May 2017, https://www.marketsandmarkets.com/Market-Reports/membrane-separation-technology-market-267308161.html?gclid=Cj0KCQjw7KqZBhCBARIsAIfTKLKMPxbTPa4edEw7H_JlbfPUgwm9dAzDU-k8rLZAo6AGhd6bIZ6hHsaAnJIEALw_wcB.
- [9] J. Zhu, J. Hou, Y. Zhang et al., “Polymeric antimicrobial membranes enabled by nanomaterials for water treatment,” *Journal of Membrane Science*, vol. 550, pp. 173–197, 2018.
- [10] L. N. Nthunya, M. F. Bopape, O. T. Mahlangu et al., “Fouling, performance and cost analysis of membrane-based water desalination technologies: a critical review,” *Journal of Environmental Management*, vol. 301, Article ID 113922, 2022.
- [11] A. Lee, J. W. Elam, and S. B. Darling, “Membrane materials for water purification: design, development, and application,” *Environmental Science: Water Research & Technology*, vol. 2, no. 1, pp. 17–42, 2016.
- [12] J. Mansouri, S. HARRISSON, and V. Chen, “Strategies for controlling biofouling in membrane filtration systems: challenges and opportunities,” *Journal of Materials Chemistry*, vol. 20, no. 22, pp. 4567–4586, 2010.
- [13] R. Xu, W. Qin, B. Zhang et al., “Nanofiltration in pilot scale for wastewater reclamation: long-term performance and

- membrane biofouling characteristics,” *Chemical Engineering Journal*, vol. 395, Article ID 125087, 2020.
- [14] J.-H. Kim, P.-K. Park, C.-H. Lee, and H.-H. Kwon, “Surface modification of nanofiltration membranes to improve the removal of organic micro-pollutants (EDCs and PhACs) in drinking water treatment: graft polymerization and cross-linking followed by functional group substitution,” *Journal of Membrane Science*, vol. 321, no. 2, pp. 190–198, 2008.
- [15] C. Ba, D. A. Ladner, and J. Economy, “Using polyelectrolyte coatings to improve fouling resistance of a positively charged nanofiltration membrane,” *Journal of Membrane Science*, vol. 347, no. 1-2, pp. 250–259, 2010.
- [16] K. Samree, P.-U. Srithai, P. Kotchaplai et al., “Enhancing the antibacterial properties of PVDF membrane by hydrophilic surface modification using titanium dioxide and silver nanoparticles,” *Membranes*, vol. 10, no. 10, Article ID 289, 2020.
- [17] F. Khoerunnisa, M. Sihombing, M. Nurhayati et al., “Poly(ether sulfone)-based ultrafiltration membranes using chitosan/ammonium chloride to enhance permeability and antifouling properties,” *Polymer Journal*, vol. 54, pp. 525–537, 2022.
- [18] P. Peer, M. Janalikova, J. Sedlarikova et al., “Antibacterial filtration membranes based on PVDF-co-HFP nanofibers with the addition of medium-chain 1-monoacylglycerols,” *ACS Applied Materials & Interfaces*, vol. 13, no. 34, pp. 41021–41033, 2021.
- [19] Committee on Challenges for the Chemical Sciences in the 21st Century, National Research Council, “Synthesis and manufacturing: creating and exploiting new substances and new transformations,” *Beyond The Molecular Frontier: Challenges for Chemistry and Chemical Engineering*, pp. 7–10, 22–30, National Academies Press, Washington, DC, 2003.
- [20] R. Kalescky, E. Kraka, and D. Cremer, “Identification of the strongest bonds in chemistry,” *The Journal of Physical Chemistry A*, vol. 117, no. 36, pp. 8981–8995, 2013.
- [21] A. Azam, A. S. Ahmed, M. Oves, M. S. Khan, and A. Memic, “Size-dependent antimicrobial properties of CuO nanoparticles against Gram-positive and -negative bacterial strains,” *International Journal of Nanomedicine*, vol. 7, pp. 3527–3535, 2012.
- [22] A. Kubacka, M. S. Diez, D. Rojo et al., “Understanding the antimicrobial mechanism of TiO₂-based nanocomposite films in a pathogenic bacterium,” *Scientific Reports*, vol. 4, Article ID 4134, 2014.
- [23] A. Sirelkhatim, S. Mahmud, A. Seeni et al., “Review on zinc oxide nanoparticles: antibacterial activity and toxicity mechanism,” *Nano-Micro Letters*, vol. 7, pp. 219–242, 2015.
- [24] P. Sikora, A. Augustyniak, K. Cendrowski, P. Nawrotek, and E. Mijowska, “Antimicrobial activity of Al₂O₃, CuO, Fe₃O₄, and ZnO nanoparticles in scope of their further application in cement-based building materials,” *Nanomaterials*, vol. 8, no. 4, Article ID 212, 2018.
- [25] Y. T. Prabhu, K. V. Rao, B. S. Kumari, V. S. S. Kumar, and T. Pavani, “Synthesis of Fe₃O₄ nanoparticles and its antibacterial application,” *International Nano Letters*, vol. 5, pp. 85–92, 2015.
- [26] M. J. Hajipour, K. M. Fromm, A. A. Ashkarran et al., “Antibacterial properties of nanoparticles,” *Trends in Biotechnology*, vol. 30, no. 10, pp. 499–511, 2012.
- [27] L. Guerrini, R. A. Alvarez-Puebla, and N. Pazos-Perez, “Surface modifications of nanoparticles for stability in biological fluids,” *Materials*, vol. 11, no. 7, Article ID 1154, 2018.
- [28] Y. Y. Loo, Y. Rukayadi, M.-A.-R. Nor-Khaizura et al., “In Vitro antimicrobial activity of green synthesized silver nanoparticles against selected Gram-negative foodborne pathogens,” *Frontiers in Microbiology*, vol. 9, Article ID 1555, 2018.
- [29] G. Franci, A. Falanga, S. Galdiero et al., “Silver nanoparticles as potential antibacterial agents,” *Molecules*, vol. 20, no. 5, pp. 8856–8874, 2015.
- [30] X.-F. Zhang, Z.-G. Liu, W. Shen, and S. Gurunathan, “Silver nanoparticles: synthesis, characterization, properties, applications, and therapeutic approaches,” *International Journal of Molecular Sciences*, vol. 17, no. 9, Article ID 1534, 2016.
- [31] S. Agnihotri, S. Mukherji, and S. Mukherji, “Size-controlled silver nanoparticles synthesized over the range 5–100 nm using the same protocol and their antibacterial efficacy,” *RSC Advances*, vol. 4, no. 8, pp. 3974–3983, 2014.
- [32] S. Tang and J. Zheng, “Antibacterial activity of silver nanoparticles: structural effects,” *Advanced Healthcare Materials*, vol. 7, no. 13, Article ID 1701503, 2018.
- [33] T. C. Dakal, A. Kumar, R. S. Majumdar, and V. Yadav, “Mechanistic basis of antimicrobial actions of silver nanoparticles,” *Frontiers in Microbiology*, vol. 7, 2016.
- [34] B. Le Ouay and F. Stellacci, “Antibacterial activity of silver nanoparticles: a surface science insight,” *Nano Today*, vol. 10, no. 3, pp. 339–354, 2015.
- [35] J. R. Morones, J. L. Elechiguerra, A. Camacho et al., “The bactericidal effect of silver nanoparticles,” *Nanotechnology*, vol. 16, no. 10, pp. 2346–2353, 2005.
- [36] I. Sur, M. Altunbek, M. Kahraman, and M. Culha, “The influence of the surface chemistry of silver nanoparticles on cell death,” *Nanotechnology*, vol. 23, no. 37, Article ID 375102, 2012.
- [37] World Health Organization, “Guidelines for drinking-water quality: fourth edition incorporating the first and second addenda,” World Health Organization, March 2022, <https://www.who.int/publications-detail-redirect/9789240045064>.
- [38] M. Azizi-Lalabadi, F. Garavand, and S. M. Jafari, “Incorporation of silver nanoparticles into active antimicrobial nanocomposites: release behavior, analyzing techniques, applications and safety issues,” *Advances in Colloid and Interface Science*, vol. 293, Article ID 102440, 2021.
- [39] H. Lu, J. Wang, M. Stoller, T. Wang, Y. Bao, and H. Hao, “An overview of nanomaterials for water and wastewater treatment,” *Advances in Materials Science and Engineering*, vol. 2016, Article ID 4964828, 10 pages, 2016.
- [40] S. A. Khan, M. Jain, A. Pandey et al., “Leveraging the potential of silver nanoparticles-based materials towards sustainable water treatment,” *Journal of Environmental Management*, vol. 319, Article ID 115675, 2022.
- [41] A. A. Yaqoob, K. Umar, and M. N. M. Ibrahim, “Silver nanoparticles: various methods of synthesis, size affecting factors and their potential applications—a review,” *Applied Nanoscience*, vol. 10, pp. 1369–1378, 2020.
- [42] R. Roto, H. P. Rasydta, A. Suratman, and N. H. Aprilita, “Effect of reducing agents on physical and chemical properties of silver nanoparticles,” *Indonesian Journal of Chemistry*, vol. 18, no. 4, pp. 614–620, 2018.
- [43] AATCC 147-2016, “Antibacterial activity assessment of textile materials: Parallel Streak method,” American Association of Textile Chemists and Colorists, 2016, https://www.techstreet.com/standards/aatcc-147-2016?product_id=1943544.
- [44] S. Zhao, W. Yan, M. Shi, Z. Wang, J. Wang, and S. Wang, “Improving permeability and antifouling performance of polyethersulfone ultrafiltration membrane by incorporation of ZnO-DMF dispersion containing nano-ZnO and

- polyvinylpyrrolidone,” *Journal of Membrane Science*, vol. 478, pp. 105–116, 2015.
- [45] A. Gul, I. Gallus, S. Sozcu, and F. Yalcinkaya, “Electrospun nanofibrous materials for oil/water separation,” in *Oil-Water Mixtures and Emulsions, Volume 1: Membrane Materials for Separation and Treatment*, pp. 41–81, ACS Publications, 2022.
- [46] N. Maximous, G. Nakhla, and W. Wan, “Comparative assessment of hydrophobic and hydrophilic membrane fouling in wastewater applications,” *Journal of Membrane Science*, vol. 339, no. 1-2, pp. 93–99, 2009.
- [47] I. M. Janah, R. Roto, and D. Siswanta, “Effect of ascorbic acid concentration on the stability of tartrate-capped silver nanoparticles,” *Indonesian Journal of Chemistry*, vol. 22, no. 3, pp. 857–866, 2022.
- [48] S. Jain, A. Jain, P. Kachhawah, and V. Devra, “Synthesis and size control of copper nanoparticles and their catalytic application,” *Transactions of Nonferrous Metals Society of China*, vol. 25, no. 12, pp. 3995–4000, 2015.
- [49] B. He, J. J. Tan, K. Y. Liew, and H. Liu, “Synthesis of size controlled Ag nanoparticles,” *Journal of Molecular Catalysis A: Chemical*, vol. 221, no. 1-2, pp. 121–126, 2004.
- [50] V. Badineni, H. Maseed, S. K. Arla, S. Yerramala, B. V. K. Naidu, and K. Kaviyarasu, “Effect of PVA/PVP protective agent on the formation of silver nanoparticles and its photocatalytic and antimicrobial activity,” *Materials Today: Proceedings*, vol. 36, Part 2, pp. 121–125, 2021.
- [51] R. Zein, I. Alghoraibi, C. Soukkarieh, M. T. Ismail, and A. Alahmad, “Influence of polyvinylpyrrolidone concentration on properties and anti-bacterial activity of green synthesized silver nanoparticles,” *Micromachines*, vol. 13, no. 5, Article ID 777, 2022.
- [52] M. F. Rabuni, N. M. N. Sulaiman, M. K. Aroua, and N. A. Hashim, “Effects of alkaline environments at mild conditions on the stability of PVDF membrane: an experimental study,” *Industrial & Engineering Chemistry Research*, vol. 52, no. 45, pp. 15874–15882, 2013.
- [53] L. M. Liz-Marzán and I. Lado-Touriño, “Reduction and stabilization of silver nanoparticles in ethanol by nonionic surfactants,” *Langmuir*, vol. 12, no. 15, pp. 3585–3589, 1996.
- [54] I. Pastoriza-Santos and L. M. Liz-Marzán, “Formation of PVP-protected metal nanoparticles in DMF,” *Langmuir*, vol. 18, no. 7, pp. 2888–2894, 2002.
- [55] A. Zielińska, E. Skwarek, A. Zaleska, M. Gazda, and J. Hupka, “Preparation of silver nanoparticles with controlled particle size,” *Procedia Chemistry*, vol. 1, no. 2, pp. 1560–1566, 2009.
- [56] T. M. D. Dang, T. T. T. Le, E. Fribourg-Blanc, and M. C. Dang, “Influence of surfactant on the preparation of silver nanoparticles by polyol method,” *Advances in Natural Sciences: Nanoscience and Nanotechnology*, vol. 3, no. 3, Article ID 035004, 2012.
- [57] A. El-Kheshen and S. F. G. El-Rab, “Effect of reducing and protecting agents on size of silver nanoparticles and their anti-bacterial activity,” *Der Pharma Chemica*, vol. 4, no. 1, pp. 53–65, 2012.